Talanta xxx (xxxx) xxxx

Contents lists available at ScienceDirect

Talanta

journal homepage: www.elsevier.com/locate/talanta

Real-time, quantitative and sensitive detection of urea by whispering gallery mode lasing in liquid crystal microdroplet

Rui Duan[a,e], Yanzeng Li[b], Bojian Shi[c], Hanyang Li[a,b,e,*], Jun Yang[d,e,**]

[a] College of Physics and Photoelectric Engineering, Harbin Engineering University, Harbin, 150001, China
[b] Department of Physics and Optical Science, University of North Carolina at Charlotte, Charlotte, NC, 28223-0001, USA
[c] Department of Physics, Harbin Institute of Technology, Harbin, 150001, China
[d] School of Information Engineering, Guangdong University of Technology, Guangzhou, 510008, China
[e] Key Lab of In-fiber Integrated Optics, Ministry Education of China, Harbin Engineering University, Harbin, 150001, PR China

ARTICLE INFO

Keywords:
Biosensor
Whispering gallery mode lasing
5CB microdroplets
Urea molecules

ABSTRACT

In this study, we demonstrate a novel nematic liquid crystal (LC) 4-cyano-4′-pentylbiphenyl (5CB) microdroplet-based biosensor for real-time, quantitative and sensitive detection of urea by whispering gallery mode (WGM) lasing technology. The single stearic acid-doped 5CB microdroplet is taken as both optical resonator and sensing reactor. To the best of our knowledge, this work is the first report of urea detection with WGM lasing. The enzymatic reaction between urea and urease produces hydroxide ions. Deprotonation and self-assembly of stearic acid occur at the aqueous/LC interface with increased pH value, promoting the reorientation of LC molecules. The detectable shift of WGM lasing spectra related to the configuration transition of LC microdroplets can be used as an indicator of enzymatic reaction, and this allows detection of urea molecules by the sensor at a concentration of only 0.1 mM. The proposed sensor also demonstrated the ability to detect urea in real urine samples. Compared with conventional POM observations, monitoring and identification of lasing spectra from LC microdroplets as a versatile method allow for more quantitative and sensitive detection of analyte reactions and can be expected to replace POM imaging technology for current LC-based biosensor systems.

1. Introduction

As the main metabolic product of protein metabolism in the human body, urea is also an important indicator for the diagnosis and clinical analysis of urinary system diseases [1–3]. The normal urea level in human urine ranges from 155 to 390 mM [4]. However, the urea content in the urine increases beyond this range as the effective filtration area of the glomerulus decreases when kidney function is impaired [5,6]. A 2018 study reported that approximately 10% of all adults suffer from chronic renal diseases, making it one of the top 20 causes of death worldwide [7]. Moreover, hepatic failure, liver cirrhosis, and toxic hepatitis decelerate urea metabolism to drive a decrease of urea in the urine [8–10]. Therefore, an improved technique to detect urea will be beneficial for early screening to allow effective preventative measures before disease outbreak, which is of great significance in clinical medicine and biochemical analysis.

In recent years, liquid crystalline materials have been widely applied in the detection of biochemical molecules such as proteins [11–14], glucose [15–17], lipid [18], heavy metal ions [19,20] and synthetic polymers [21–23], due to the amplification and transmission of biochemical events at the aqueous/LC interface. pH-sensitive LC microdroplet sensors have become one of the representatives of LC biosensors. In the study of urea detection, Khan et al. attempted to covalently immobilize urease by PAA-b-LCP, and achieved a urea detection limit as low as 3 mM by using POM image recognition [6]. Liu et al. also visually detected the urease hydrolysis of urea according to changes in the optical textures of hemispherical LC microdroplets [24]. However, these LC microdroplet-based sensors are used only to estimate the biochemical reaction process. To date, a great number of the detector readouts are currently based on the bare-eye observation of the optical appearance under a POM. In these sensing modalities, the reaction process is difficult to be quantitatively and accurately characterized, thereby limiting the further development of the LC sensing device in real-time monitoring.

Here, to address these limitations, we propose to use WGM lasing in LC microdroplets to perform real-time quantitative monitoring of the

* Corresponding author. Key Lab of In-fiber Integrated Optics, Ministry Education of China, Harbin Engineering University, Harbin, 150001, PR China.
** Corresponding author.
E-mail addresses: hanyang_li@qq.com (H. Li), yangj@gdut.edu.cn (J. Yang).

https://doi.org/10.1016/j.talanta.2019.120513
Received 18 August 2019; Received in revised form 22 October 2019; Accepted 26 October 2019

reaction process of analyte. Due to their nearly perfect spherical structure and exceptionally smooth surface, LC microdroplets can be used as a great optical microcavity to achieve WGM lasing [25–27]. In principle, the excitation light from a gain medium undergoes multiple total internal reflections at the optical microcavity interface and then gets resonance amplification due to constructive interference [28]. The resonance frequency of microcavity relies upon the refractive index distribution along the propagation path of light. In turn, changes in the refractive index can be detected by the WGM spectra in the form of a resonance frequency shift as well [29].

With the unique properties of LC materials, WGM lasing in LC microdroplet is expected to become a promising tool in the field of biosensing. Some advantages of this method include i) WGM lasing can transform the biochemical reaction process into a spectral response in real-time, providing more accurate and quantitative information; ii) the overall arrangement of LC molecules in microdroplets is highly sensitive to the type and strength of the local molecules anchoring at the LC/aqueous interface, so any tiny changes in the anchoring state of LC molecules will be captured by the WGM resonance spectra in real-time; iii) the large surface-area-to-volume ratio of LC microdroplets allows the full reaction of molecules at the LC/aqueous interface and helps to improve the detection limit.

Herein, we used stearic acid as a functional material, and exploited the highly efficient enzymolysis of urea by urease for urea detection. Stearic acid is a saturated fatty acid molecule, contains a long hydrophobic chain and a hydrophilic head group [30]. During the enzymatic hydrolysis of urea, OH^- ions are released, resulting in an increase in the local pH value. Thus deprotonation and self-assembly of carboxylic acid then occur at the aqueous/LC interface, leading to anchoring transition of 5CB molecules from planar (Fig. 1a) to homeotropic (Fig. 1b) anchoring. In the meantime, the director configuration of LC microdroplet transforms correspondingly from bipolar to radial. In our work, the mechanism of lasing was unambiguously identified by comprehensive spectroscopic analysis and attributed to WGMs. The detectable shift of WGM lasing spectra can be used as an indicator of enzymatic reaction and allows detection of urea molecules by the sensor at a concentration of only 0.1 mM, which is lower than the detection limit of currently available urea sensor based on LC materials.

2. Experimental

2.1. Materials

Nematic liquid crystal 4-cyano-4′-pentylbiphenyl (5CB), stearic acid (Grade I, > 98.5%), urea, urease, n-Heptane (anhydrous), thiourea, hydroxyurea, acetamide, and *N*, *N*-Dimethylformamide, were purchased from Sigma-Aldrich. Potassium phosphate monobasic and potassium phosphate dibasic, which are used to prepare phosphate buffer solution (PBS) with different pH values, were purchased from Aladdin. 4-dicyanomethylene-2-methyl-(6-4-dimethylaminostryl)-4*H*-pyan (DCM), serving as the gain media, was purchased from Exciton. All aqueous solutions used in our work were prepared with deionized (DI) water using a Milli-Q system (Millipore, USA).

2.2. Preparation of experimental solution

All enzymatic aqueous solutions were prepared in PBS. To test the selectivity of the sensor, a mixture of 1 mM urea and 0.1 mg/ml urease was pre-incubated at 37 °C for 30 min. Urine samples, obtained from a healthy volunteer, were filtered through sterile 0.1 mm pore filters to remove protein aggregates and other bulky impurities. The original urine sample was diluted 100-, 200-, 500-, 1000-, 2000-, 5000-fold dilutions with deionized water and stored in a reagent bottle for reserve. The urea concentration of above six groups of samples was determined by standard method in the clinical chemistry laboratory of Harbin Engineering University Hospital, as shown in Supporting Information Table S1.

2.3. Preparation of 5CB sample

The 5CB (1% v/v) doped with stearic acid and DCM dye was first dissolved in anhydrous heptane. The concentration of doped stearic acid and DCM were 0.1 wt% and 0.05 wt% of 5CB, respectively. Then the 5CB sample was ultrasonically treated for 30 min. After evaporating the organic solvent, the sample was transferred to a small reagent bottle for standby application.

2.4. Preparation of 5CB microdroplets

Instead of sophisticated processing procedures, the 5CB microdroplets in our experiment were self-assembled and fabricated by straightforward techniques. First, a home-made microtube with a diameter of 7 μm was prepared via flame heated taper-drawing technique using silica capillary tubing (100 μm inner diameter, 162 μm outer diameter), as shown in Supporting Information Fig. S1. Next, a side of the conical microtube was connected to a pump-controlled microchannel for extraction of the 5CB samples prepared previously. Finally, by controlling the pumping status, the required sizes of 5CB microdroplets were generated in an immiscible environment (Supporting Information Fig. S2). We used the microtube to “capture” and

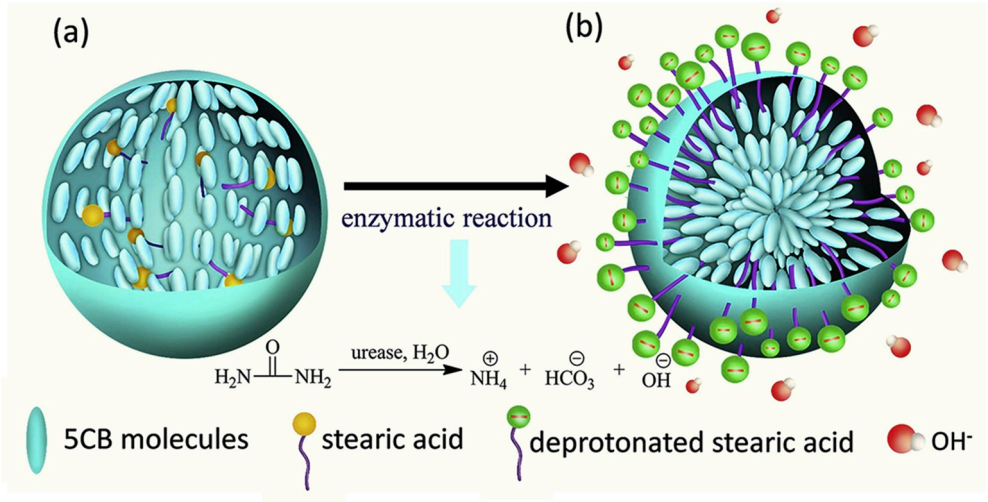

Fig. 1. Schematic illustration of the structural transition of stearic acid-doped 5CB microdroplet from planar anchoring (a) to homeotropic anchoring (b).

manipulate microdroplets. To do this, the microdroplets were suspended from the end of the microtube rather than connected to the microtube to prevent any interference with the experimental results from pressure fluctuations in the microtube. It needs to be explained that in order to facilitate the excitation of WGM lasing, LC microdroplets in experiments are generated and controlled by a home-made microtube, and only one microdroplet can be generated at a time. Therefore, only POM images of single LC microdroplets were presented in each photo. Each group of experiments was repeated at least five times to avoid false-positive results.

2.5. WGM lasing spectral measurement

Fig. S3 in Supporting Information shows a schematic diagram of our experimental setup. The WGM lasing spectra of the stearic acid-doped 5CB microdroplets were measured by a spectrometer (PG2000, Ideaoptics Technology Ltd., China). Optical images of microdroplets were obtained with a polarized light microscope (POM, BX43P, Olympus, Japan). A CCD camera (DP21, Olympus, Japan) was used to record the POM images of the stearic acid-doped 5CB microdroplets.

3. Results and discussion

3.1. WGM spectral responses of stearic acid-doped 5CB microdroplets with various pH

Disturbance on the LC microdroplet surface due to the anchoring of chemical and biological molecules can disrupt the balance between the elastic free energy and the surface anchoring energy of the microdroplet, resulting in alteration of its internal orientation structure [31]. Therefore, the 5CB doped with function molecules sensitive to the external environment can show high application value in various LC-based sensors [32].

We first investigated the orientation properties of stearic acid-doped 5CB microdroplets with various pH. Microdroplets of the same diameter (65 μm) were produced in PBS with different pH values, and the POM images were recorded after 30 min (Fig. 2a). The results showed that for pH value was lower than 7, all the LC microdroplets presented bipolar configuration, indicating that 5CB molecules were parallel to the surface of the microdroplets. We speculate that this phenomenon is attributable to the low concentration of OH^- ions in PBS, which does not deprotonate a sufficient amount of stearic acid molecules to alter the droplet structure. When the pH value of PBS was 7.4, there was an obvious disclination loop on the surface of the microdroplets (Fig. 2 a (5) and Supporting Information Fig. S4); and the LC microdroplets presented axial configuration (a typical transition state between bipolar to radial configuration) [33]. As the pH value was gradually increased, the disclination loop on the surface gradually shrank to a hedgehog point defect and a radial configuration emerged. For pH value of 9, the radial configuration became fairly perfect. We attribute these phenomena to the increasing density of deprotonated stearic acid, inducing the spontaneous transformation of 5CB molecules from parallel to perpendicular anchoring.

Next, we ran a controlled trial to confirm that the structural changes of the LC microdroplets were indeed caused by the doping of stearic acid. To do this, same-diameter microdroplets without stearic acid were prepared in the pH range of 4–10. All the LC microdroplets exhibited bipolar configuration and their state remained unchanged for at least 40 min (Supporting Information Fig. S5). Furthermore, the effects of DCM dye on any structural changes in the microdroplets were also eliminated experimentally, and the LC microdroplets obtained at different pH values were similar to those shown in Fig. 2a (Supporting Information Fig. S6).

The initial configuration of LC microdroplets for sensing is typically bipolar or radial. Once LC microdroplets in the two configurations are obtained, excitation and observation of WGM lasing in LC microdroplets can be performed. In our experiments, considering the use of pump light source (532 nm) and the need for good solubility and stability of dyes in LC materials, we chose DCM as the gain dye [25,34]. The DCM doped in 5CB microdroplets produces broad-spectrum fluorescence when stimulated by pumping light. Some of the fluorescence that meets the resonance conditions would return to the same point in phase, resulting in resonance amplification, so sharp WGM lasing peaks are formed in the spectra. A schematic diagram of the lasing experimental setup is shown in Fig. 2b. The 532 nm pump light was guided to the surface of 5CB microdroplet via a fiber tip. A drop of PBS was deposited on a PMMA substrate to serve as the microdroplet's host medium. To test this design, we conducted a series of experiments to analyze and verify the characteristics of WGM lasing in acid-doped 5CB microdroplets from the lasing threshold, mode number and Q factor (see verification of WGM lasing characteristics in the Supporting Information for details).

Furthermore, the WGM spectral response of acid-doped 5CB microdroplets was studied at different pH values. To prevent degradation of the dye molecules, the microdroplets were only excited for a short period of time (about 1 s) to record the spectra. Therefore, the laser-induced thermal effect was not observed in the experiments. We first generated stearic acid-doped 5CB microdroplets in PBS with pH = 7 (inset (1) and (3) in Fig. 2c). Then, 40 μL of NaOH with a pH of 7.4 was added into the sensing system. A clear disclination loop appeared in the POM image of the microdroplet (inset (2) and (4) in Fig. 2c). A shift of 0.59 nm was produced during the 1–4 min response time. The blue shift of WGM lasing is due to the decrease of refractive index along the direction of the electric field oscillation of TE polarization mode (see wavelength shift mechanism of WGM lasing in the Supporting Information for details). Subsequently, we repeated the above process and measured the temporal response of WGM wavelength shift with different pH, as shown in Fig. 2d. We found that the wavelength shift of WGM increased with the increase of pH, but this effect saturated at about pH = 8.6 (Fig. 2e). At lower pH values ($7 \leq pH \leq 8.6$), the spectral response exhibited an approximately linear response to pH value (inset in Fig. 2e). Thus, a quantitative relationship between pH value and WGM wavelength shift was established. The experiments revealed a sensitivity of 1.56 nm/pH (defined as the slope of the calibration curve). It is worth noting that stearic acid-doped 5CB microdroplets exhibit the same radial state but different spectral shift behavior when the pH values of the added NaOH are 8.2 and 8.6, respectively. This indicates that more detailed information (i.e., tiny structural changes in droplets that cannot be identified by the naked eye) can be obtained by using WGM spectral response. Therefore, the proposed sensing system can achieve accurate detection of solutions with weakly alkaline pH ($7 \leq pH \leq 8.6$). The system also has a great application for the potential detection of pH-related biochemical molecules, such as urea, glucose [17], catalase [35], penicillin [36], and cholesterol [37].

3.2. Urea detection limit

After determining the WGM spectral response of acid-doped LC microdroplet at different pH values, the detection performance of the sensor for biochemical molecules was further studied. Under the catalysis of urease, urea may be hydrolyzed into ammonia, which can subsequently be hydrolyzed into an ammonium ion and hydroxyl ion, increasing the ambient pH. Therefore, we first investigated the orientation properties of acid-doped 5CB microdroplets at the reaction solution/LC interface.

Stearic acid-doped microdroplets with 65 μm diameter were prepared in PBS with a urease concentration of 0.1 mg/ml, and then a small amount of urea solution (40 μL of 10 mM concentration urea, almost 1/5 of the PBS volume) was introduced. Fig. 3a shows POM images of the microdroplet evolution. After 1 min, topological point defects emerged at the edges of the bipolar LC microdroplets. Within

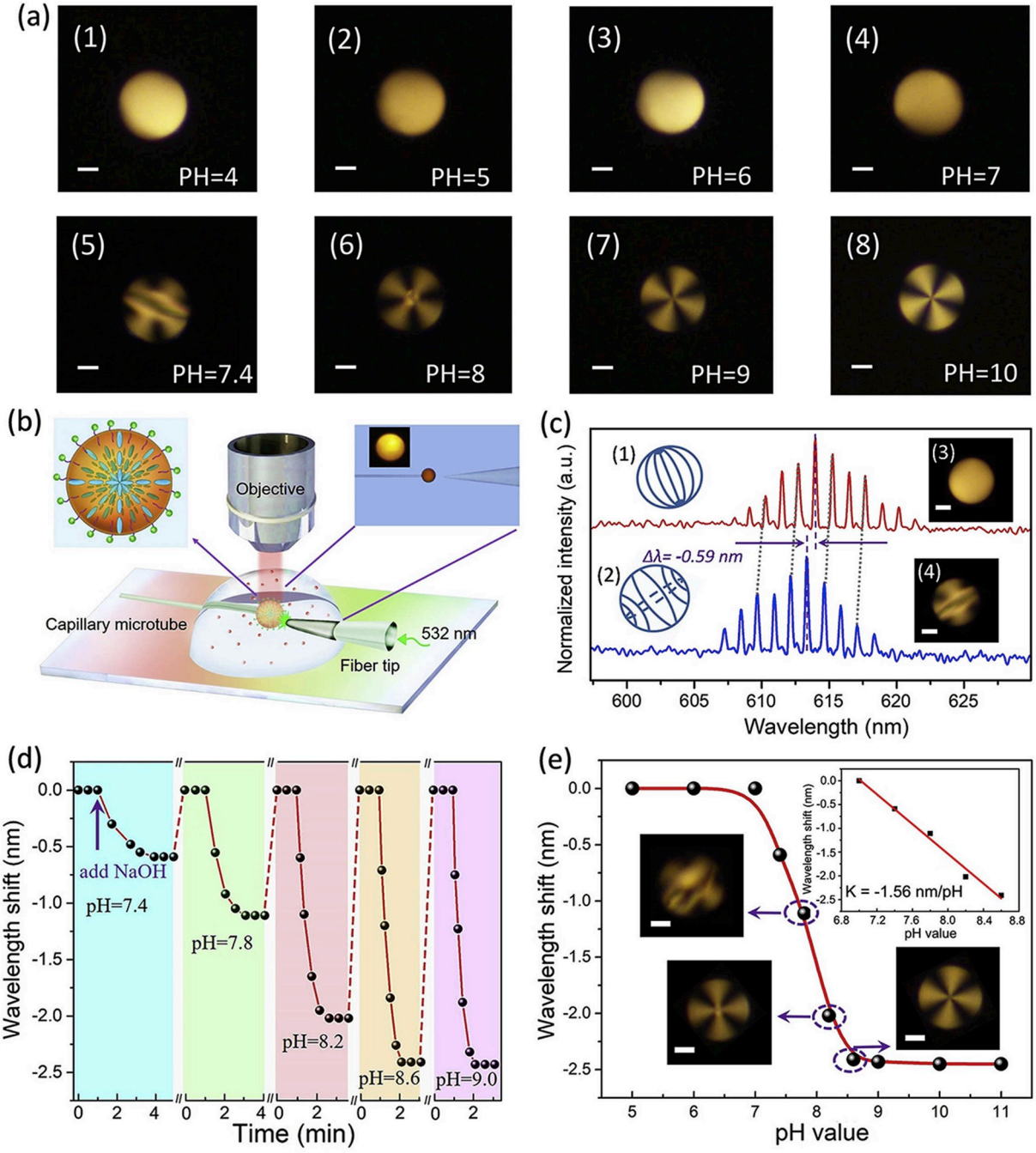

Fig. 2. (a) POM images of acid-doped 5CB microdroplets in PBS with different pH. Scale bars 20 μm. (b) Schematic diagram of WGM lasing experimental setup. The 532 nm pump light was guided to the surface of 5CB microdroplet via a fiber tip. (c) WGM lasing spectra of stearic acid-doped 5CB microdroplet before (red line) and after (blue line) addition of NaOH at pH = 7.4. Schematic illustrations of corresponding configurations within 5CB microdroplets are illustrated in insets (1) and (2), respectively. POM images of corresponding configurations are illustrated in insets (3) and (4), respectively. (d) Temporal dependence of WGM wavelength shift with different pH. The results of five different pH values are presented in their separate independent regions. (e) Wavelength shift of WGM lasing spectra as a function of pH value of NaOH. Inset: within a certain pH range (7 ≤ pH ≤ 8.6), the spectral response exhibited an approximately linear response to pH value. (For interpretation of the references to colour in this figure legend, the reader is referred to the Web version of this article.)

4 min, LC microdroplets gradually experienced escaped radial and pre-radial configurations [33]. By 5 min, LC microdroplets had formed a stable radial configuration. A clear crisscross pattern and point defect in the center of the microdroplets were observed.

In order to initially determine the detection limit of the sensor for urea, we repeated the above experiment with urea at a concentration of 1 mM. As shown in Fig. 3b, LC microdroplets formed a stable radial configuration within 11 min and the state remained unchanged for 40 min. Fig. S7 in Supporting Information showed the entire evolution of microdroplet as observed by POM images. Unlike with the use of a high concentration (10 mM) of urea, disclination loops were observed in the intermediate state. The radial configuration could not form when the detected urea concentration was decreased to 0.1 mM (Fig. 3c). This suggests the OH^- ions produced in the urease-catalyzed hydrolysis cannot support enough carboxylic acid molecules to deprotonate. A urea concentration of 0.01 mM was also tested, and the microdroplet configuration did not change within 40 min (data not shown).

To accurately and quantitatively describe the urease-catalyzed

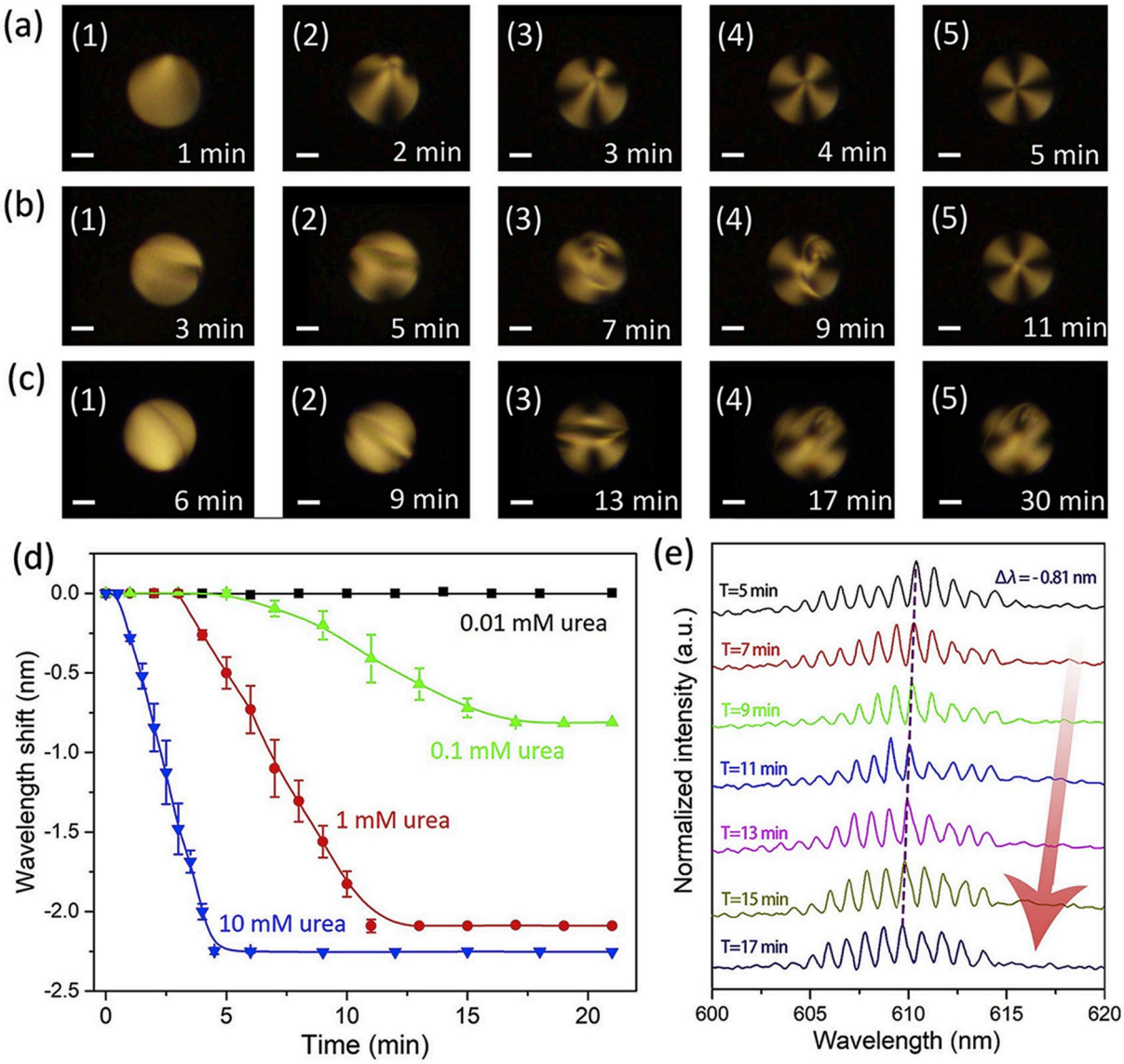

Fig. 3. POM images of 65-μm-diameter acid-doped 5CB microdroplets in PBS (pH = 7) containing 0.1 mg/ml urease after addition of 40 μL of 10 mM (a), 1 mM (b), 0.1 mM (c) urea. Scale bars 20 μm. (d) Temporal dependence of WGM wavelength shift with different urea concentrations. (e) Portion of WGM lasing spectra as a function of time. Spectra were collected from a 65-μm-diameter acid-doped 5CB microdroplet in PBS containing 0.1 mg/ml urease after adding 40 μL 0.1 mM urea.

Table 1
Comparison of performance of different LC biosensors for urea detection.

Type of technique	Type of sensing structure	Detection limit	Sensitivity	Reference
Optical pattern-based LC sensor	Planar	5 mM	–	[38]
Optical pattern-based LC sensor	Spherical	3 mM	–	[6]
Optical pattern-based LC sensor	Hemispheric	0.5 M	–	[24]
WGM lasing-based LC sensor	Spherical	0.1 mM	8.1 nm/mM	Present work

hydrolysis of urea, we further analyzed the WGM spectral responses of the acid-doped 5CB microdroplets during hydrolysis. The spectral changes at different concentrations of urea under the hydrolysis of 0.1 mg/ml urease were recorded, as shown in Fig. 3d. Our experimental results indicate the proposed urea sensor exhibited a detection limit of 0.1 mM, which was better than the detection limit of urea by the current LC sensor reported. WGM spectra had a blueshift of 0.81 nm within 5–17 min at this urea concentration (Fig. 3e). The detection performance of the resulting biosensor is compared with other reported LC biosensors, and the results are summarized in Table 1. The detector readout of our system is based on the monitoring of WGM spectral responses in LC microdroplets, without the needs of imaging and image analysis. Shifts in WGM spectra associated with microdroplet configuration changes can be used as an effective indicator of enzymatic reaction. The detection limit of urea by WGM lasing-based LC sensor is at least one order of magnitude lower than that based on optical pattern of LC. In addition, due to the double amplification effect of LC molecules and WGMs, the maximum sensitivity in our demonstration is 8.1 nm/mM for urea molecules. It is worth noting that for detected urea concentrations of 10 mM and 1 mM, the LC microdroplets exhibited the same radial state but different spectral shift behavior. This suggests that the use of WGM spectral response to detect the reaction process is more accurate than simple POM observations by the naked eye.

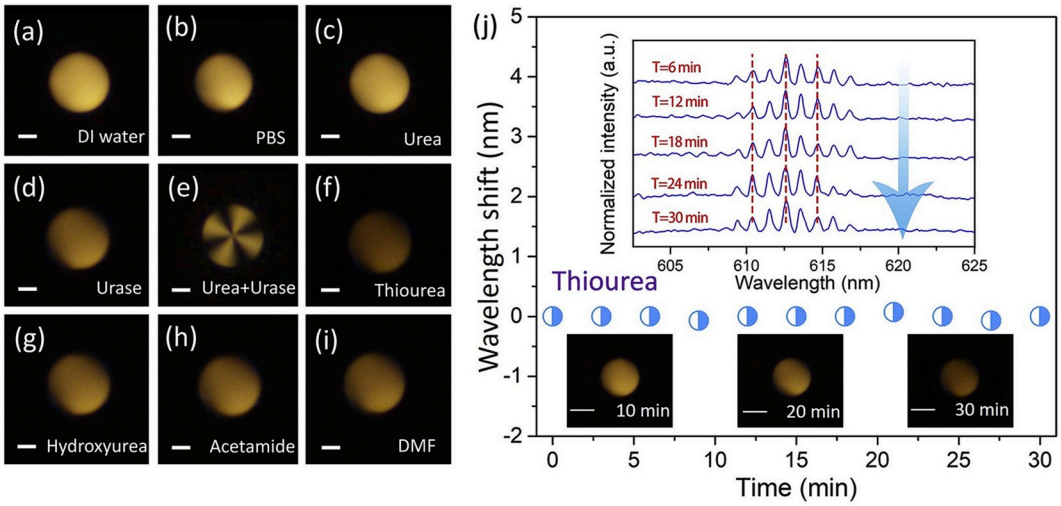

Fig. 4. POM images (recorded after 30 min) of 65-μm-diameter acid-doped 5CB microdroplets in DI water (a), pure PBS (pH = 7) (b), PBS (pH = 7) containing 10 mM urea (c), 0.1 mg/ml urase (d), urease and urea mixture (e), 10 mM thiourea (f), 10 mM hydroxyurea (g), 10 mM acetamide (h), 10 mM *N*,*N*-Dimethylformamide (DMF) (i). Scale bars 20 μm. (j) Temporal dependence of WGM wavelength shift with thiourea. Inset: corresponding WGM lasing spectra and POM images.

3.3. The specificity of urea sensor

In order to confirm that the observed changes in microdroplet structure were indeed caused by the release of OH^- ions during urease-catalyzed hydrolysis of urea, we prepared stearic acid-doped 5CB microdroplets with the same diameter in DI water, PBS (pH = 7), urea solution (concentration 10 mM), and urease solution (concentration 0.1 mg/ml), respectively. We found that all of the 5CB microdroplets remained in a bipolar configuration for at least 40 min (Fig. 4a–d). However, the microdroplets generated in the mixture of urea and urease showed radial configuration (Fig. 4e). Based on these results, we confirmed that the release of OH^- ions in the enzymatic reaction caused changes in the pH of the external environment, promoted the deprotonation of stearic acid molecules, and induced the reassembly of LC molecules in the microdroplets.

In the detection of urea, sensors are highly susceptible to interference from other chemical substances with structures similar to urea molecules. Therefore, we next tested the response characteristics of a series of structural analogs of urea (Supporting Information Fig. S8), as shown in Fig. 4f–i. The sensor demonstrated excellent specificity for urea, and the LC microdroplets exhibited the same bipolar configuration in the four selected analogs. The results for thiourea are presented as an example, and the WGM lasing spectra in the reaction process are presented in Fig. 4j. There was no shift during a 30 min monitoring period.

3.4. Urine sample analysis

We next performed urea testing on six groups of urine samples to demonstrate the practical potential of the proposed WGM lasing-based LC sensor. Temporal dependence of WGM wavelength shift with urine sample under six different dilutions was measured as summarized in Fig. 5a, where the error bars were calculated according to the standard deviation of four tests for each concentration. As expected, the final equilibrium shift and wavelength change rate of WGM spectral response decrease with the increase of dilution. With the increase of urea dilution, the concentration of OH^- ions produced by enzymatic hydrolysis decreases. Low density deprotonated stearic acid is not enough to induce a complete change of anchoring state of 5CB molecules. The POM images with different dilutions can be used as an evidence for the above explanation, as shown in the inset of Fig. 5b.

It is important to study the interfering effects of biological sample matrixes for accurate detection of target molecules [39,40]. To do this, six groups of pure urea solutions were prepared in DI water with the same concentration as urea in urine samples. The WGM spectral response of pure urea samples as reference was studied by the same experimental procedure, as shown in Fig. 5b and Supporting Information Table S2. It is clear that the reference samples have different spectral shifts from the urine samples, indicating that the impurities interfere with the test results. But fortunately, the detection mechanism of the sensor is specific hydrolysis of urea by urease, so the impurities in the urine cannot be hydrolyzed, which reduces the interfering effects on the experimental results to some extent. Despite a few interfering effects from sample matrixes, this novel WGM lasing-based LC sensing system still exhibits the ability to detect urea in real urine samples at present.

4. Conclusions

In this study, we developed an acid-doped 5CB microdroplet biosensor for real-time, quantitative and sensitive detection of urea molecule by WGM lasing technology. The single stearic acid-doped 5CB microdroplet was taken as both optical resonator and sensing reactor. Benefit from the double amplification of the 5CB molecules and WGM resonance, the signals of the biological reaction at the interface were significantly enhanced. More importantly, the detectable shift of WGM lasing spectra related to the configuration transition of LC microdroplets can be used as an indicator of enzymatic reaction. The proposed sensor can detect urea at a concentration as low as 0.1 mM, which is better than the detection limit of urea by the current LC sensor reported. It also exhibited the ability for detection of real human urine samples. Compared with conventional POM observations, monitoring and identification of lasing spectra from LC microdroplets as a versatile method allow for more quantitative and sensitive detection of analyte reactions and can be expected to replace conventional POM observations.

Declaration of competing interest

There are no conflicts to declare.

Acknowledgments

This work was supported by the National Key Research and Development Program of China (2016YFF0200704 and

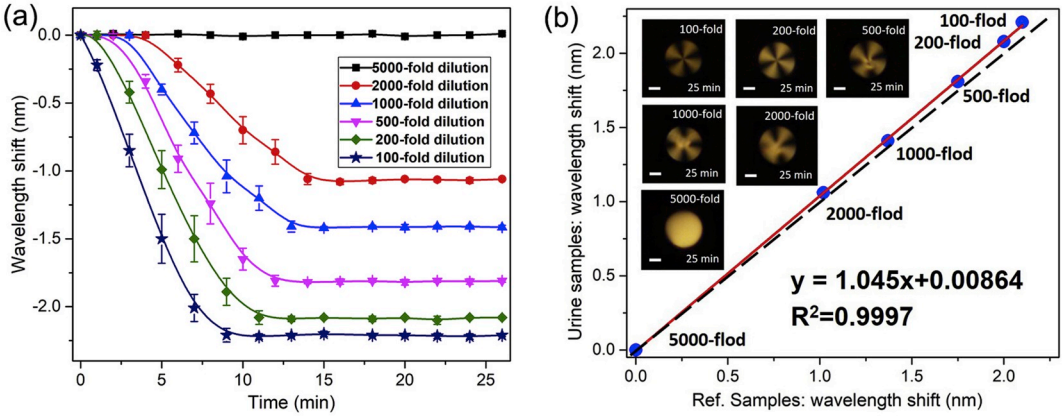

Fig. 5. (a) Temporal dependence of WGM wavelength shift with different-fold dilutions of urine. All experiments were conducted four times. (b) Comparison of WGM spectral shift between reference samples and urine samples. The dashed line corresponds to ideality and the solid one is the regression of the comparison data. Inset: POM images (recorded after 25min) of acid-doped 5CB microdroplets in urine sample under 100-, 200-, 500-, 1000-, 2000-, 5000-fold dilutions. Scale bars 20 μm.

2017YFB0405502) and the National Natural Science Foundation of China (61635007 and 11474072).

Appendix A. Supplementary data

Supplementary data to this article can be found online at https://doi.org/10.1016/j.talanta.2019.120513.

References

[1] D. Aronson, M.A. Mittleman, A.J. Burger, Elevated blood urea nitrogen level as a predictor of mortality in patients admitted for decompensated heart failure, Am. J. Med. 116 (2004) 466–473.
[2] E. Coll, A. Botey, L. Alvarez, E. Poch, L. Quintó, A. Saurina, M. Vera, C. Piera, A. Darnell, Serum cystatin C as a new marker for noninvasive estimation of glomerular filtration rate and as a marker for early renal impairment, Am. J. Kidney Dis. 36 (2000) 29–34.
[3] R. Bellomo, J.A. Kellum, C. Ronco, Acute kidney injury, Lancet 380 (2012) 756–766.
[4] M. Mascini, G.G. Guilbault, Urease coupled ammonia electrode for urea determination in blood serum, Anal. Chem. 49 (1977) 795–798.
[5] T.W. Meyer, T.H. Hostetter, Uremia, N. Engl. J. Med. 357 (2007) 1316–1325.
[6] M. Khan, S.Y. Park, General Liquid-crystal droplets produced by microfluidics for urea detection, Sens. Actuators, B 202 (2014) 516–522.
[7] G.B. Piccoli, M. Alrukhaimi, Z.H. Liu, E. Zakharova, A. Levin, What we do and do not know about women and kidney diseases; questions unanswered and answers unquestioned: reflection on World Kidney Day and International Woman's Day, BMC Nephrol. 19 (2018) 66.
[8] C. Ronco, R. Bellomo, A. Brendolan, M. Dan, P. Piccinni, G.L. Greca, Effects of different doses in continuous veno-venous haemofiltration on outcomes of acute renal failure: a prospective randomised trial, Lancet 355 (2000) 26–30.
[9] I. Bozgeyik, M. Senel, E. Çevik, M.F. Abasıyanık, A novel thin film amperometric urea biosensor based on urease-immobilized on poly (N-glycidylpyrrole-co-pyrrole), Curr. Appl. Phys. 11 (2011) 1083–1088.
[10] J.O. Clemmesen, J. Kondrup, L.B. Nielsen, F.S. Larsen, P. Ott, Effects of high-volume plasmapheresis on ammonia, urea, and amino acids in patients with acute liver failure, Am. J. Gastroenterol. 96 (2001) 1217–1223.
[11] V.K. Gupta, J.J. Skaife, T.B. Dubrovsky, N.L. Abbott, Optical amplification of ligand-receptor binding using liquid crystals, Science 279 (1998) 2077–2080.
[12] Y.Y. Luk, M.L. Tingey, K.A. Dickson, R.T. Raines, N.L. Abbott, Imaging the binding ability of proteins immobilized on surfaces with different orientations by using liquid crystals, J. Am. Chem. Soc. 126 (2004) 9024–9032.
[13] J. Zhang, X. Su, D. Yang, C. Luan, Label-free liquid crystal biosensor for cecropin B detection, Talanta 186 (2018) 60–64.
[14] Y. Wang, L. Zhou, Q. Kang, L. Yu, Simple and label-free liquid crystal-based sensor for detecting trypsin coupled to the interaction between cationic surfactant and BSA, Talanta 183 (2018) 223–227.
[15] M. Khan, S.Y. Park, Liquid crystal-based proton sensitive glucose biosensor, Anal. Chem. 86 (2014) 1493–1501.
[16] S. Zhong, C.H. Jang, Highly sensitive and selective glucose sensor based on ultraviolet-treated nematic liquid crystals, Biosens. Bioelectron. 59 (2014) 293–299.
[17] J. Kim, M. Khan, S.Y. Park, Glucose sensor using liquid-crystal droplets made by microfluidics, ACS Appl. Mater. Interfaces 5 (2013) 13135–13139.
[18] J.M. Brake, M.K. Daschner, Y.Y. Luk, N.L. Abbott, Biomolecular interactions at phospholipid-decorated surfaces of liquid crystals, Science 302 (2003) 2094–2097.
[19] S. Yang, C. Wu, H. Tan, Y. Wu, S. Liao, Z. Wu, G. Shen, R. Yu, Label-free liquid crystal biosensor based on specific oligonucleotide probes for heavy metal ions, Anal. Chem. 85 (2013) 14–18.
[20] C.H. Chen, Y.C. Lin, H.H. Chang, S.Y. Lee, Ligand-doped liquid crystal sensor system for detecting mercuric ion in aqueous solutions, Anal. Chem. 87 (2015) 4546–4551.
[21] M.I. Kinsinger, B. Sun, N.L. Abbott, D.M. Lynn, Reversible control of ordering transitions at aqueous/liquid crystal interfaces using functional amphiphilic polymers, Adv. Mater. 19 (2007) 4208–4212.
[22] M.I. Kinsinger, M.E. Buck, N.L. Abbot, D.M. Lynn, Immobilization of polymer-decorated liquid crystal droplets on chemically tailored surfaces, Langmuir 26 (2010) 10234–10242.
[23] D.Y. Lee, J.M. Seo, W. Khan, J.A. Kornfield, Z. Kurjib, S.Y. Park, pH-responsive aqueous/LC interfaces using SGLCP-b-polyacrylic acid block copolymers, Soft Matter 6 (2010) 1964–1970.
[24] D. Liu, C.H. Jang, A new strategy for imaging urease activity using liquid crystal droplet patterns formed on solid surfaces, Sens. Actuators, B 193 (2014) 770–773.
[25] Y. Wang, H. Li, L. Zhao, Y. Liu, S. Liu, J. Yang, Tunable whispering gallery modes lasing in dye-doped cholesteric liquid crystal microdroplets, Appl. Phys. Lett. 109 (2016) 231906.
[26] Y. Lu, Y. Yang, Y. Wang, L. Wang, J. Ma, L. Zhang, W. Sun, Y. Liu, Tunable liquid-crystal microshell-laser based on whispering-gallery modes and photonic band-gap mode lasing, Opt. Express 26 (2018) 3277–3285.
[27] L. Zhao, Y. Wang, Y. Yuan, Y. Liu, S. Liu, W. Sun, J. Yang, H. Li, Whispering gallery mode laser based on cholesteric liquid crystal microdroplets as temperature sensor, Opt. Commun. 402 (2017) 181–185.
[28] A.M. Armani, R.P. Kulkarni, S.E. Fraser, R.C. Flagan, K.J. Vahala, Label-free, single-molecule detection with optical microcavities, Science 317 (2007) 783–787.
[29] R. Stoian, B.K. Lavine, A.T. Rosenberger, pH sensing using whispering gallery modes of a silica hollow bottle resonator, Talanta 194 (2019) 585–590.
[30] G.R. Han, C.H. Jang, Detection of heavy-metal ions using liquid crystal droplet patterns modulated by interaction between negatively charged carboxylate and heavy-metal cations, Talanta 128 (2014) 44–50.
[31] D.S. Miller, X. Wang, N.L. Abbott, Design of functional materials based on liquid crystalline droplets, Chem. Mater. 26 (2014) 496–506.
[32] R.J. Carlton, J.T. Hunter, D.S. Miller, R. Abbasi, P.C. Mushenheim, L.N. Tan, N.L. Abbott, Chemical and biological sensing using liquid crystals, Liq. Cryst. Rev. 1 (2013) 29–51.
[33] I.-H. Lin, D.S. Miller, P.J. Bertics, C.J. Murphy, J.J. de Pablo, N.L. Abbott, Endotoxin-induced structural transformations in liquid crystalline droplets, Science 332 (2011) 1297–1300.
[34] P.R. Hammond, Laser dye DCM, its spectral properties, synthesis and comparison with other dyes in the red, Opt. Commun. 29 (1979) 331–333.
[35] Q.Z. Hu, C.H. Jang, Using liquid crystals for the label-free detection of catalase at aqueous–LC interfaces, J. Biotechnol. 157 (2012) 223–227.
[36] X. Bi, H. Deny, K.L. Yang, Real-time liquid crystal pH sensor for monitoring enzymatic activities of penicillinase, Adv. Funct. Mater. 19 (2009) 3760–3765.
[37] H.G. Lee, S. Munir, S.Y. Park, Cholesteric liquid crystal droplets for biosensors, ACS Appl. Mater. Interfaces 8 (2016) 26407–26417.
[38] M. Khan, Y. Kim, J.H. Lee, I.K. Kang, S.Y. Park, Real-time liquid crystal-based biosensor for urea detection, Anal. Methods 6 (2014) 5753–5759.
[39] H.X. Zhang, J.B. Chen, X.F. Guo, H. Wang, H.S. Zhang, Highly sensitive determination of nitric oxide in biologic samples by a near-infrared BODIPY-based fluorescent probe coupled with high-performance liquid chromatography, Talanta 116 (2013) 335–342.
[40] X. Xie, A.A. Suleiman, G.G. Guilbault, Determination of urea in serum by a fiber-optic fluorescence biosensor, Talanta 38 (1991) 1997 – 1200..